aaps PharmSciTech

Table of contents

Medendorp J, Lodder RA. Acoustic-Resonance Spectrometry as a Process Analytical Technology for Rapid and Accurate Tablet Identification. *AAPS PharmSciTech*. 2006; 7 (1): Article 25. DOI: 10.1208/pt070125

Acoustic-Resonance Spectrometry as a Process Analytical Technology for Rapid and Accurate Tablet Identification

Joseph Medendorp[1] and Robert A. Lodder[1]

[1]Department of Pharmaceutical Sciences, College of Pharmacy, A123 ASTeCC Building 0286, Lexington, KY 40536

Correspondence to:

Robert A. Lodder

Tel: (859) 257-9232

Fax: (859) 257-2489

Email: Lodder@uky.edu

Submitted: August 4, 2005; Accepted: December 29, 2005; Published: March 17, 2006

Abstract

This research was performed to test the hypothesis that acoustic-resonance spectrometry (ARS) is able to rapidly and accurately differentiate tablets of similar size and shape. The US Food and Drug Administration frequently orders recalls of tablets because of labeling problems (eg, the wrong tablet appears in a bottle). A high-throughput, nondestructive method of online analysis and label comparison before shipping could obviate the need for recall or disposal of a batch of mislabeled drugs, thus saving a company considerable expense and preventing a major safety risk. ARS is accurate and precise as well as inexpensive and nondestructive, and the sensor is constructed from readily available parts, suggesting utility as a process analytical technology (PAT). To test the classification ability of ARS, 5 common household tablets of similar size and shape were chosen for analysis (aspirin, ibuprofen, acetaminophen, vitamin C, and vitamin B12). The measures of successful tablet identification were intertablet distances in nonparametric multidimensional standard deviations (MSDs) greater than 3 and intratablet MSDs less than 3, as calculated from an extended bootstrap error-adjusted single sample technique. The average intertablet MSD was 65.64, while the average intratablet MSD from cross-validation was 1.91. Tablet mass (r^2 = 0.977), thickness (r^2 = 0.977), and density (r^2 = 0.900) were measured very accurately from the AR spectra, each with less than 10% error. Tablets were identified correctly with only 250 ms data collection time. These results demonstrate that ARS effectively identified and characterized the 5 types of tablets and could potentially serve as a rapid high-throughput online pharmaceutical sensor.

Keywords: Sound, chemometrics, pharmaceuticals, process analytical technology (PAT), integrated sensing and processing (ISP)

Introduction

On December 4, 2003, the US Food and Drug Administration recalled 504 bottles of mislabeled Magno-Humphries, Inc, Dixon's, Acetaminophen, 325 mg Analgesic Tablets.[1] A rapid, nondestructive online method of analysis and comparison with labeling could have prevented the recall and disposal of the batch of mislabeled acetaminophen, thus sparing the company considerable cost and a major safety risk. Process analytical technology (PAT)

encompasses the design and development of processes to guarantee a predefined quality of pharmaceutical materials at the end of the manufacturing process, as warranted by risk analysis.[2] These processes come in various forms, including multivariate data acquisition and analysis tools, and in-process and endpoint monitoring tools. With the PAT system in effect, it becomes possible to implement real-time product release and increase pharmaceutical automation, thus providing the environment for significant reduction in manufacturing and labeling accidents.

Acoustic-resonance spectrometry (ARS) is an underutilized PAT that could become an analytical method of choice for the physical characterization of some analytes in pharmaceutical manufacturing. The wide-ranging measurements that can be made by ARS include sample compaction and axial strain, deformation, hydration and drying endpoint, elasticity, molecular stacking, and homogeneity, making ARS a very descriptive method of sample analysis.[3] In addition, ARS provides a rapid and efficient way to nondestructively identify and quantify an analyte with no sample preparation.[4] It has thus far successfully analyzed tablets,[4-6] powders,[7-10] and semisolids and liquids,[7,11,12] and it has quantified bulk moisture levels in otherwise identical samples.[4] Unlike most methods of analysis using photons, in ARS acoustic waves penetrate centimeters or even meters of material. Currently, the industry standard for tablet characterization and identification is high performance liquid chromatography (HPLC), which, in addition to requiring extensive preparation (tablet grinding, dissolution, and extraction), destroys the tablet during the analytical process.[13,14] Only a few samples are collected from each batch for HPLC analysis, but entire batches must be disposed of if there are a few failed samples. Through chemometrics, near-infrared (NIR) and acoustic spectrometry are now making their way into the pharmaceutical industry as alternatives to HPLC testing.[15,16] Though the identification of specific functional groups from AR spectra is beyond the scope of this research, ARS can easily be applied to the quantification of active pharmaceutical ingredient (API) or moisture in tablets because of the high correlation between AR spectral features and chemical composition. Chemical changes lead to changes in physical characteristics such as density, compressibility, and acoustic velocity. For example, the density of acetaminophen is 1.2083 g/mL, while the density of aspirin is 1.3571 g/mL. The velocity of sound, therefore, is much higher in aspirin than it is in acetaminophen, resulting in a different set of acoustic interactions between each tablet and the quartz rod. These different interactions permit the extraction of bulk physical properties from the AR spectra and the characterization of even subtle correlated chemical differences between tablet groups. The chemical/physical relationship linkage can also be exploited to differentiate between unique formulations of the same API, as numerous constituents

contribute to the final formulation, including excipients, compression aids, binders, coatings, disintegrants, and emulsifying agents.

Vibrational techniques such as NIR and infrared spectroscopy are very sensitive to the presence of water. In fact, water's absorption is so strong that it often overwhelms other signals of interest.[17] Much computation can be required to correct for or deconvolve spectra with a large water absorption to extract other useful features.[17-23] Acoustic waves are not necessarily as sensitive to the presence of water and do not suffer from the same limited penetration depth in water that causes problems in the NIR. ARS can be used along with NIR spectrometry to decrease interferences from water and increase the range of analytes that can be determined with good sensitivity.[24] The last few years have seen the advent of commercial instruments for acoustic analysis of liquid and semisolid samples.[25] Thus, this technology is rapidly gaining popularity for the physical characterization of analytes.

Sound is a longitudinal wave—one whose compressions and rarefactions oscillate parallel to the direction of propagation.[26] When an acoustic wave is applied to a sample, the medium responds by locally expanding and contracting, with particles in the medium drawing closer together and moving farther apart. The degree to which a particular medium responds is a product of its bulk modulus, or simply, its incompressibility. For dense materials with very little compressibility, a sound wave propagates very rapidly, while for less dense samples, sound travels more slowly.

Figure 1 shows a schematic of the AR spectrometer used for the following discussion. In the absence of a tablet at the vertex of the quartz rod, the applied acoustic signal received at the detector is a standing wave that is characteristic of the quartz wave guide. When a tablet comes in contact with the rod, the acoustic waves propagate through the tablet/quartz interface and pass to the tablet holder (which may contain a second transmitting transducer). Waves are transmitted through the tablet or reflected back through the tablet, where they reenter the quartz rod. The 2 sound paths lead to a pattern of in-phase and out-of-phase interferences (between the standing wave traveling through the quartz rod from piezoelectric transducer (PZT) to PZT with no tablet interaction, and the wave propagating through the tablet) that is characteristic of the tablet.[27] This phenomenon is illustrated in an animation in Figure 2. The quartz rod was chosen as the means of propagation because the speed of sound is significantly larger in the rod than in the tablet; thus, the difference in delay time between the reference channel and the tablet channel is maximized. A rod composed of quartz also helps keep acoustic impedance to a minimum, according to $Z_{ac} = P/(vA)$, where Z_{ac} is acoustic

impedance, *P* is pressure (which is proportional to the wave amplitude), *v* is the velocity of the sound wave, and *A* is a unit of area.[26]

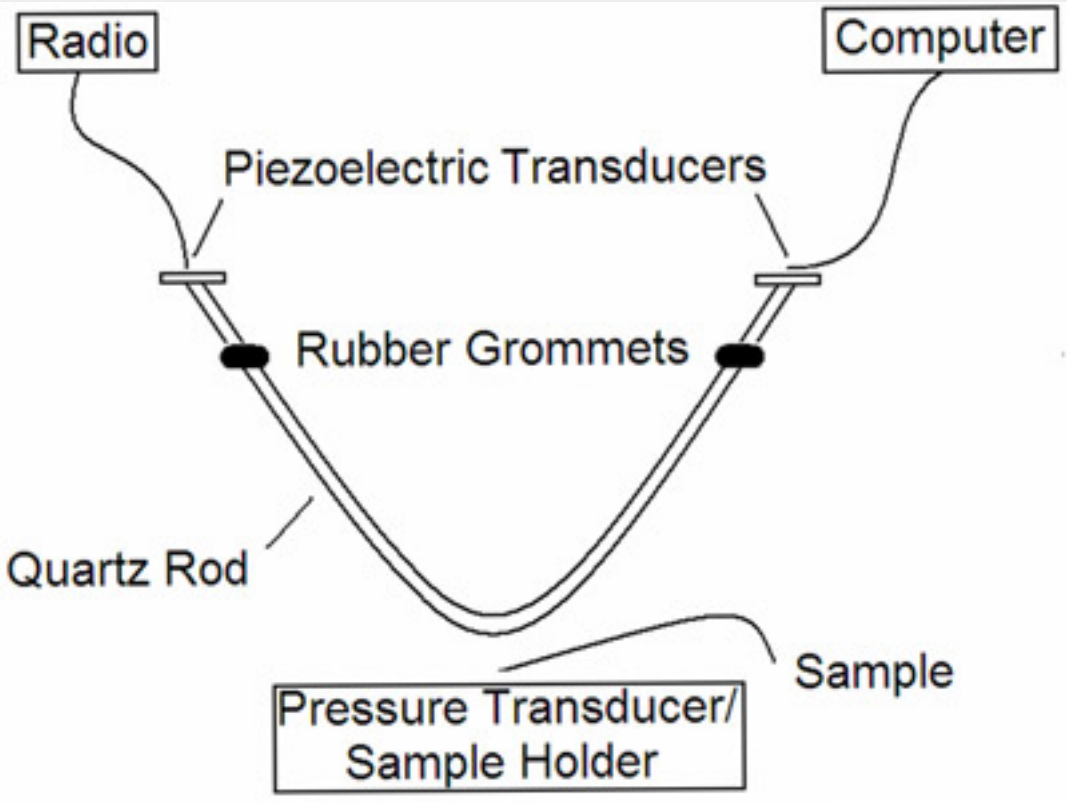

Figure 1. Acoustic-resonance spectrometer schematic illustrating the instrumentation. The piezoelectric transducer on the left receives the excitation signal from the radio, while the one on the right receives the transmitted signal through the quartz rod.

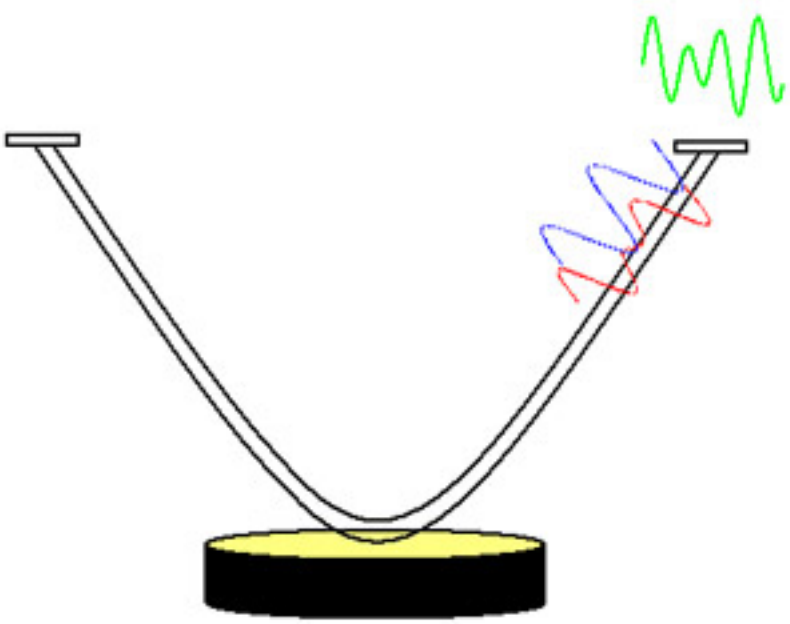

Figure 2. Animation demonstrating the principle by which the acoustic-resonance spectrometer operates. In the absence of a sample, excitation of the rod results in a standing wave and a consistent frequency spectrum. In the presence of a sample, a second sound path is introduced, passing through the sample and reflecting off the sample holder, and recombining with the original standing wave. This results in an entirely new wave, the interference pattern from the combination of frequencies from the standing wave and the sample wave.

The next-generation AR spectrometer, which is already in construction and testing, will use integrated sensing and processing (ISP), encoding the excitation signal source so the detector output is directly proportional to the analyte concentration or classification (such an excitation signal is also called an ISP waveform). When the most distinguishing frequencies are preselected for excitation, the ISP excitation source can be an encoded weighted frequency spectrum, eliminating the need for postcollection computation and simplifying the AR spectrometer for use as a PAT sensor. Thus, an ISP excitation waveform is one in which each frequency in the frequency-domain representation of the waveform is weighted (typically between +1 and –1) so that the sum of the signals over the frequency and the integration time is proportional to the property of interest. ISP has demonstrated significantly reduced analysis times compared with the full-spectrum approach and appears to perform consistently with full-spectrum ARS for analyte separation and API quantification.[5,7] The utility in the ISP approach

lies in its ease of application. For example, to differentiate between 2 visually indistinguishable groups of tablets, one can download from an online database an ISP waveform that is a prerecorded MP3 file written to distinguish between the required tablets. The final PAT sensor can be very simple when the waveform is recorded to a CD or an MP3 player and “played” through the tablets.

The current work represents a step in the direction of ISP-ARS. This research was performed to test the hypothesis that an AR spectrometer using ISP-compatible waveforms is able to rapidly and accurately differentiate tablets of similar size and shape. An ISP-compatible waveform is an excitation signal in which each frequency in the frequency-domain representation of the waveform is weighted +1. In an ISP calibration process, the calibration samples are usually tested first with an ISP-compatible waveform to determine the distinguishing frequencies for the actual ISP encoded waveform. In this research, an FM radio receiver supplies one source of broadband random excitation for ARS. Such a waveform could easily be recorded in MP3 format or on a CD for use in a high-throughput PAT sensor.

The ultrasound literature indicates that buffer rods (steel, aluminum, quartz, etc) coupled to PZTs are commonly used as probes to monitor various online processes, including fabrication of microfluidic devices,[28] polymer processing,[29] and inline die casting.[30] A typical industrial tablet press is capable of pressing slightly more than one tablet per punch station per second.[31] Each punch station can easily be fitted with a PZT, much like the buffer rod probe. With one second per punch, there is ample time to collect an acoustic signal from the tablet as it is being punched. Such technology would be capable of testing 100% of the tablets passing down the manufacturing line; therefore, no scale-up would be required to reach production rates. Thus, ARS is a high-throughput assay suitable for 100% product testing.

Theory

AR spectra collected at *n* frequencies can be expressed as points in an *n*-dimensional hyperspace. These spectra usually form complex patterns in that hyperspace as analyte concentration changes because of the nonlinear nature of acoustic interactions.[32] Nevertheless, a plot of canonical correlation coefficients calculated from the principal component scores shown in Figure 3 illustrates that spectra from similar tablets tend to cluster in the same region of hyperspace.[33,34] However, to prove this assertion more quantitatively, the bootstrap error-adjusted single sample technique (BEST) nonparametric cluster analysis algorithm can be employed, and multidimensional standard deviations (MSDs) between

clusters and spectral data points can be calculated.[35] To calculate the distances in MSDs, a population **P** is created as an *m* × *n* matrix in hyperspace **R** whose rows are the individual samples and columns are the frequencies. BEST considers each frequency from a spectrum of *n* frequencies to be taken as a separate dimension.[36] **P*** is a discrete realization of **P** based on a calibration set **T** of the same dimensions as **P***. This realization is chosen one time from **P** to approximate all possible sample variations present in **P**. **P*** has parameters **B** and **C**, where **C =** E**(P)** and **B** is the Monte Carlo approximation to the bootstrap distribution. The expectation value, E**(P)**, is the center of **P**, and **C** is a row vector with the same number of rows as there are columns in vector **P**. New test spectra **X** are projected into **R** containing **B**; rows of **B** are mapped onto a vector connecting **C** and **X**. **C** and **X** have the same dimensions. The integral over **R** is calculated from the center of **P** in all directions. A skew-adjusted MSD is based on the comparison of the expectation value **C =** E**(P)** and **C =** med**(T)**, the median of **T** in hyperspace projected onto the hyperline connecting **C** and **X**. The result is an asymmetric MSD that provides 2 measures of the MSD along the hyperline connecting **C** and **X**. Equation 1 defines the MSD in the direction of **X**, and Equation 2 defines the MSD in the opposite direction. Skew-adjusted MSDs can be used to calculate mean distances between spectra of different samples.

$$+ \sigma \bullet | \int 0 + \sigma (\int R P^{*} \rightarrow (C X \rightarrow) \int R P^{*} \rightarrow (C X \rightarrow) = 0.34 \quad (1)$$

$$- \sigma \bullet | \int 0 - \sigma (\int R P^{*} \rightarrow (C X \rightarrow) \int R P^{*} \rightarrow (C X \rightarrow) = 0.34 \quad (2)$$

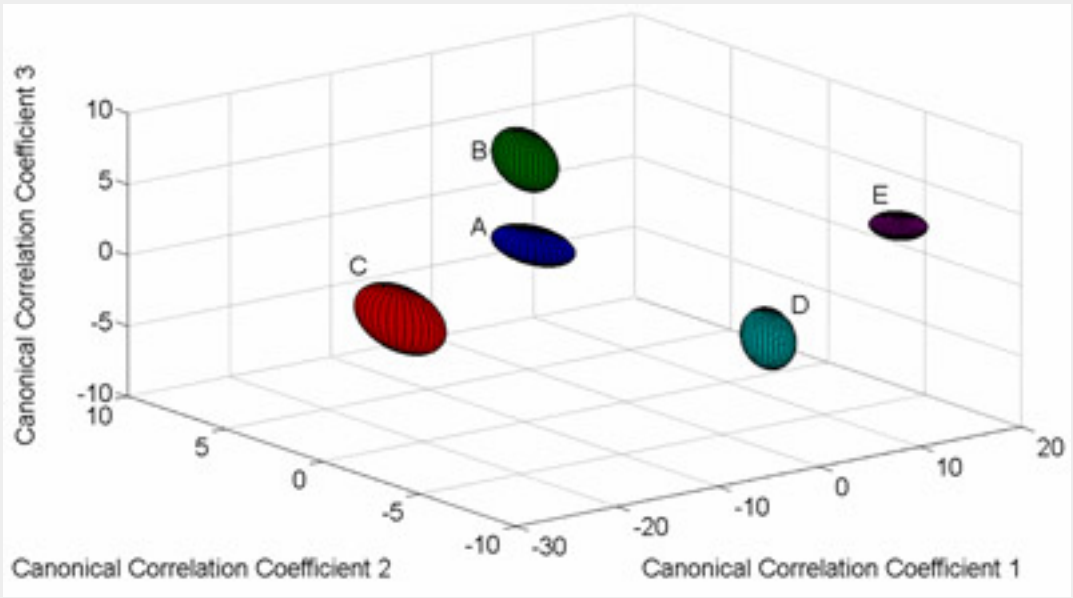

Figure 3. The first 3 canonical correlation coefficients calculated from the principal component scores from the radio receiver noise source. Ellipses are drawn 3 SDs from the center of the clusters. (A) Ibuprofen, (B) aspirin, (C) acetaminophen, (D) vitamin B_{12}, and (E) vitamin C.

Materials and Methods

A simple schematic of the instrument is shown in Figure 1, and an animated illustration of its operation is shown in Figure 2.[4,37,38] The acoustic range was limited to 0 to 4 kHz in the computational model for experiments to ensure compatibility with the simple ISP strategy. Three different broadband acoustic noise sources were tested: a radio receiver (Model D-3150, Consumer Electronics Corp, Knoxville, TN) tuned to a local unused frequency (94.9 MHz FM); a white noise–generating Zener diode amplifier circuit constructed for these experiments[39]; and a function generator (FG) (Model DS335, Stanford Research Systems, Sunnyvale, CA). The PZTs (CUI Inc, Beaverton, OR) were connected directly to the audio-amplifier leads inside the receiver, and because of the magnitude of the receiver signal, no pre- or postamplification was necessary. Ideally, a white noise generator creates equal excitation at each frequency in its spectral range. However, even in the case of the best possible applied white noise, the PZTs responded much better at some frequencies than at others. The receiver and Zener white noise generators were compared with an FG programmed to output a swept 10 V signal from 10 Hz to 4 kHz in steps of 10 Hz. The following discussion concentrates on a brief comparison of the 2 most effective methods of generating the noise excitation, the FG and the FM receiver. Typical Fourier transform spectra of the received signal from both methods are shown in Figure 4. Spectra appear different in the 2 methods because the FG sweeps a signal from 10 Hz to 4 kHz in discrete steps of 10 Hz, while the FM receiver delivers essentially random noise excitation across the entire range from 0 to 4 kHz. Because the overall magnitudes of the signals per unit time at the receiving PZT were comparable for the 2 methods, the FG had to deliver a much more intense excitation per unit time at each of its frequencies, which increased the acoustic nonlinearities caused by mechanical interface discontinuities in the sampling system. To more effectively illustrate the distinctions between AR tablet spectra, we have provided Figure 5, which shows second derivatives of the logarithms calculated from the Fourier transform of the radio data.

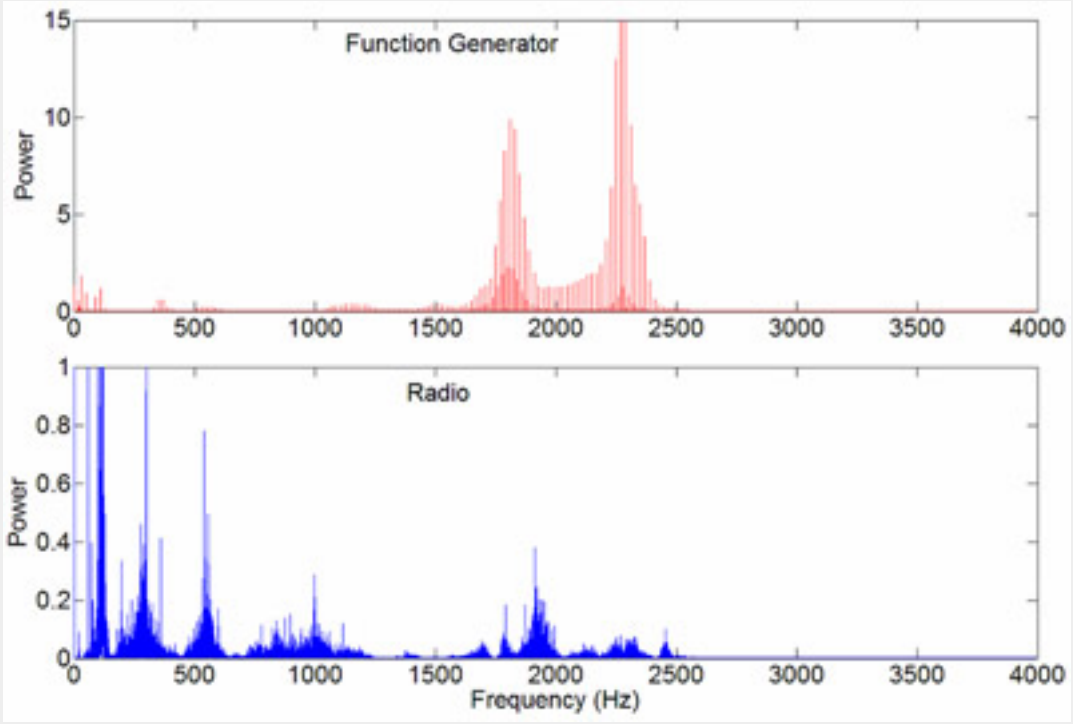

Figure 4. Fourier transform spectra comparison of the received signals between the function generator and the radio.

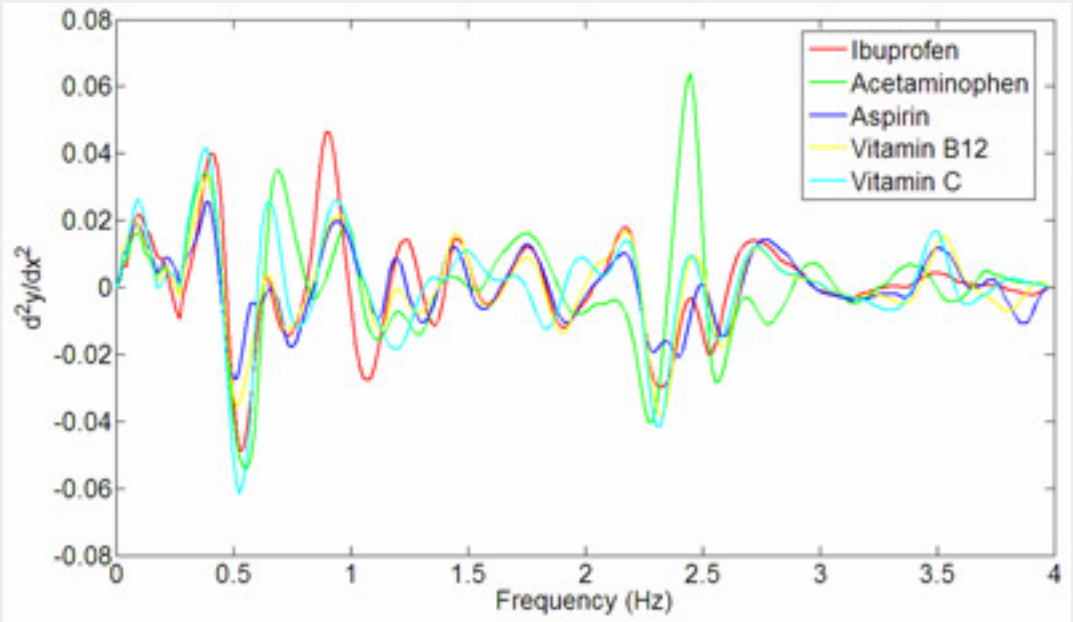

Figure 5. Log and second derivatives calculated from the Fourier transform radio data to better illustrate the differences between the tablet groups.

The vertex of the quartz rod was in mechanical contact with the sample, causing it to resonate with the rod. Tablet samples were mounted on a scale (Model 3120, Health O Meter, Bridgeview, IL) to ensure that the pressure on each sample was consistent and reproducible.

The PZT detector output signal was collected via a 16-bit soundcard (Realtek AC97, Realtek Semiconductor Japan Corp, Yokohama, Kanagawa, Japan) for processing and analysis in Matlab 7.0.1 (Mathworks Co, Natick, MA). For each sample, 15 seconds of data were collected at a sample rate of 8 kHz and a Fourier transform was calculated. Using the spectra of the blank (quartz rod), a signal-to-noise ratio of 50:1 was calculated by dividing the magnitude of the largest peak by the SD of its replicates. With the sample rate of 8 kHz, the maximum frequency collected was 4 kHz, though there was very little signal above 2.5 kHz.

The objective of the initial experiment was to prove that the selected tablets of similar size and shape could be differentiated unequivocally. Tablets used were ibuprofen (Perrigo, Allegan, MI), acetaminophen (Leiner Health Products, Carson, CA), aspirin (Wal-Mart Stores, Inc, Bentonville, AR), vitamin C (Leiner Health Products), and vitamin B_{12} (Weider Nutrition Group, Salt Lake City, UT). To effectively capture small variations and inconsistencies inherent to different tablets, we scanned 10 tablets from each group. The instrument was configured so the quartz rod applied 100 g of pressure to each tablet for the duration of the scan. To eliminate any effects of instrument drift on the analysis, we scanned tablets in random order. Each tablet was removed from the sample holder prior to replicate scans, and the quartz rod was raised and repositioned between each scan.

Tablet mass was determined with a digital mass balance (Mettler BB244, Mettler Instrument Corp, Hightstown, NJ), thickness was measured to ±0.1 mm with a vernier caliper, and volume for density measurements were determined by water displacement. Figure 6 demonstrates the correlation between acoustic spectra and these physical properties. For initial data analysis, principal components and canonical correlation coefficients were calculated from the spectral data. Principal components were calculated by a singular value decomposition of matrix **A** according to Equation 3:

$$A = U S V \quad (3)$$

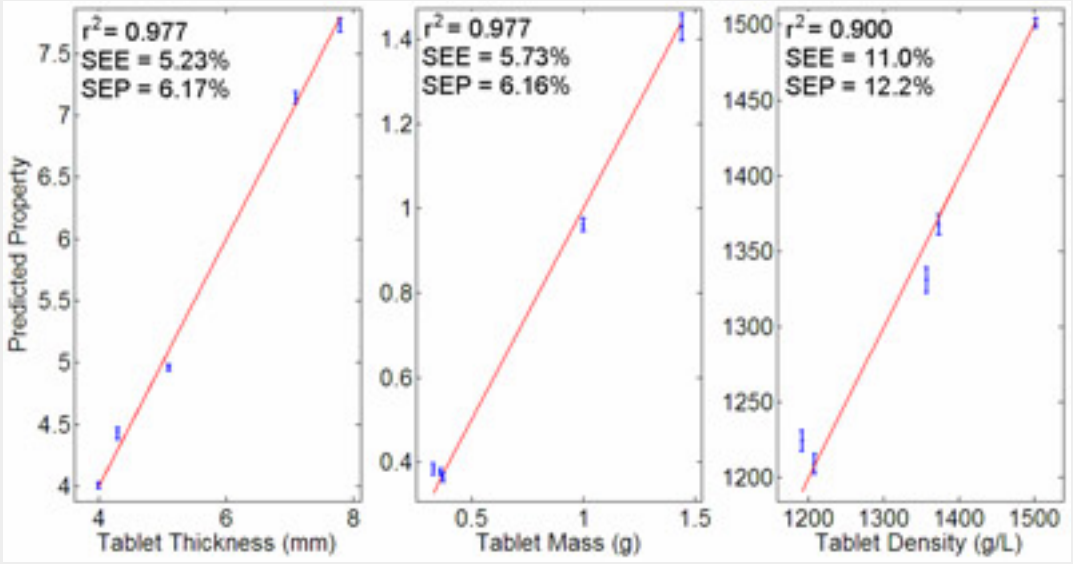

Figure 6. Cross-validation results demonstrating the ability of acoustic-resonance spectrometry to predict tablet thickness, mass, and density from the acoustic-resonance spectra of the tablets.

where **A** is the matrix of original spectra, **U** is the matrix of eigenvalues (scores), **S** is a diagonal matrix of singular values, and **V** is the matrix of eigenvectors (loadings).

In Equation 4, a multiple linear regression of **U** indicates which of the components has the strongest correlation to tablet thickness, mass, or density, *y*, where *a* is the y-intercept, *b* is a vector of regression coefficients, and *c* is the residual.

$$y = a + b\,U + c \tag{4}$$

These components were used in a leave-one-out cross-validation to determine how effectively ARS predicted these physical properties from their acoustic spectra according to Equation 5, where σ^2 is the variance and $f_i(U_i)$ is the prediction of the model for the *i-th* pattern *m* in the training set, after it has been trained on the *m-1* other patterns.

$$\sigma\,\mathrm{LOO} \bullet 2 = 1\,m \sum i = 1\,i = m\,(\,y\,i - f\,i\,(\,U\,i\,)\,)\,2 \tag{5}$$

These physical properties have a tightly knit relationship, so their individual effects on acoustic spectra need not be isolated for the purposes of the following discussion. Using a multidimensional translation of tablet populations, we established the dynamic range of the

ARS instrument for each of the properties listed above.[35]

To estimate detection limits for dynamic range calculations, AR spectra between tablet groups (intertablet spectra) from the 2 tablet populations ($\mathbf{P_1}$ and $\mathbf{P_2}$) with the smallest MSD separation (aspirin and ibuprofen) were used as $m \times n$ matrices.[35] The columns of the matrices were averaged by Equations 3 and 4, giving two $1 \times n$ vectors.

$$P1ave = 1m \sum i = 1i = m P1i \quad (6)$$

$$P2ave = 1m \sum i = 1i = m P2i \quad (7)$$

A difference spectrum $\mathbf{X}$ was calculated from $\mathbf{P_{2ave}} - \mathbf{P_{1ave}}$. One population was spatially translated toward the other, $\mathbf{P_{Adjusted}} = \mathbf{y} * \mathbf{X} + \mathbf{P_2}$, where $\mathbf{y}$ (defined on the interval $\{0 < y \leq 1\}$) started at 0 and increased in increments of 0.01 until $\mathbf{P_1}$ and $\mathbf{P_{Adjusted}}$ were inseparable. To estimate the smallest possible tablet thickness, mass, and density differences that could still be separated, the fraction of the final spatial translation was multiplied by the difference in physical properties.[35] The procedure was conducted separately using the 2 tablet groups with the smallest MSD separation (ibuprofen and aspirin) and the two tablet groups with the largest MSD separation (acetaminophen and vitamin C).

In addition to ARS data, NIR data were collected from tablets, for comparison. Spectra from 1100 to 2500 nm were collected with an NIR spectrometer (Technicon InfraAlyzer 500, Tarrytown, NY) interfaced to a computer (OptiPlex GXM 5166, Dell, Round Rock, TX) running SESAME 3.1 (Bran+Luebbe, Norderstedt, Germany). The data set consisted of 50 tablets, 10 of each type as listed above. To reduce room noise, external interferences, and thermal detector drift, the tablets were scanned inside the instrument drawer and scanned in random order. All NIR data were also exported to Matlab 7.0.1 for processing and analysis.

Results

The BEST MSDs for the AR spectra are shown in Table 1. The average intertablet MSD for the AR spectra using receiver-generated noise was 65.44, and the average for the FG was 38.65. Leave-one-out cross-validations were calculated to quantify the intratablet variation (variation in AR spectra for multiple scans of the same type of tablet). A distance in MSDs between a tablet and a spectral data cluster that is less than 3 is defined as inseparable (a 99.8% confidence limit). The average cross-validation MSDs were 1.92 for the receiver-generated

noise and 2.2 for the FG, suggesting that the receiver-generated noise was better for maximizing intertablet variation and minimizing intratablet variation. While the FG and the radio provided different excitation signals, the magnitudes of the total integrated signals at the receiving PZT at any given time were comparable between the 2 methods. Therefore, the FG had to deliver a much larger excitation at each of its individual frequencies as the frequency was swept. Because of small mechanical interface discontinuities between the PZTs and the quartz rod, and between the rod and the samples, the larger excitation signal with the FG produced more acoustic nonlinearity effects in the spectra. This suggests that a CD/MP3 player with an excitation signal specifically tailored to match the frequencies and amplitudes of the most distinguishing spectral features will also be more effective than an FG. NIR spectrometry (with a 120-second sample scan integration time) provided a median MSD intertablet separation of 363.55 and a median intratablet separation of 1.96. These results suggest that NIR spectra are superior to AR spectra in differentiating among the tablet classes. However, it should be noted that the NIR integration time was almost 10× greater than the ARS integration time, so the distances in MSDs should be almost 3× greater for NIR spectrometry than for ARS based on the integration time alone. In many process sensing applications, the fact that NIR spectrometry produces slightly better results will not justify the much higher cost of using it. It should be noted that both NIR spectrometry and ARS were perfectly accurate in all of their tablet classifications.

Table 1. BEST MSDs Between the Tablet Groups for the FM Receiver and the FG*

MSDs	Ibu	APAP	Asp	Vit B_{12}	Vit C
FM Radio					
Ibu	**2.33**	62.29	13.82	74.82	77.61
APAP		**1.78**	50.08	77.34	105.22
Asp			**1.76**	74.77	83.57
Vit B_{12}				**1.95**	36.94
Vit C					**1.76**
FG					
Ibu	**2.88**	62.32	24.10	29.24	31.77
APAP		**2.52**	47.49	45.76	75.73

Asp	**1.80**	16.65	39.26
Vit B_{12}		**1.74**	14.21
Vit C			**2.07**

*Intragroup tablet MSDs are shown across the diagonal. APAP indicates acetaminophen; asp, aspirin; BEST, bootstrap error-adjusted single sample technique; FG, function generator; ibu, ibuprofen; MSDs, nonparametric multidimensional standard deviations; Vit, vitamin.

The strong correlation between AR spectra and tablet thickness, mass, and density is illustrated in Figure 6. ARS predicted tablet thickness with r^2 = 0.977, a standard error of estimate (SEE) of 5.23%, and a standard error of performance (SEP) of 6.17%. ARS predicted tablet mass with r^2 = 0.977, SEE = 5.73%, and SEP = 6.16%, and ARS predicted tablet density with r^2 = 0.900, SEE = 11.0%, and SEP = 12.2%. NIR spectrometry only slightly outperformed ARS for these measurements, with average leave-one-out cross-validation r^2 = 0.998, SEE = 1.30%, and SEP = 1.40% (data not shown).

Discussion

Versatility and Flexibility of ARS

ARS provides an extremely versatile instrument for PAT. The same instrument and chemometrics can be applied to multiple sample types, including powders,[7-10] semisolids, and liquids.[7,11,12] Because of the large difference in acoustic velocities between a quartz rod and a sample, there is no practical minimum physical sample size required for this instrument to function. The rod and excitation can always be scaled to the physical sample size. While the excitation frequencies passing through the rod and the sample are the same, because of the difference in acoustic velocity, the waveforms are almost always longer in the quartz. The sample pathlength is always longer than the reference pathlength. Regardless of the sample size, the waveforms will never be perfectly in phase as they recombine at the detector on the rod. This will result in a characteristic pattern of constructive and deconstructive interferences for every analyte in response to the difference in thickness. Additionally, when samples' API and formulations differ chemically, the differences have physical manifestations in such qualities as mass, density, and compressibility, and these are observed in the AR spectra.

Speed of Method

A short experiment was conducted to determine the minimum scan time at which the radio receiver ARS was still capable of separating tablets. Tablets were scanned again for 15 seconds. Rather than calculating the Fourier transform from the time domain data in its entirety, we calculated the FFT from the first 1 second and from the first 250 ms of data. Principal components and BEST MSDs were calculated from the shorter data sets and plotted to verify that tablet groups were still separable by the same success metrics. For 1 second of time domain data, the average intertablet MSD was 29.30 and the average intratablet MSD was 1.768. For 250 ms of time domain data, the average intertablet MSD was 19.51 and the average intratablet MSD was 1.71. These results suggest that although having 15 seconds of data collection offers an advantage in separation, it is not necessary to collect more than 250 ms, an obvious advantage in PAT.

Freedom From Interferences

The main sources of potential interference for the AR spectrometer in this configuration are (1) RF cross-talk directly between PZTs, (2) acoustic waves that propagate through the instrument's support structures, (3) spontaneous additional noise bursts in the receiver (this source of interference is unlikely in the FG), and (4) inconsistent sample placement due to the manual loading procedure. Studies were conducted to identify and quantify these effects, which we will discuss individually. First, to assess the possibility of RF cross-talk, a PZT was suspended 10 cm from the epoxy-fastened receiving PZT; the 2 PZTs had no mechanical contact. A white noise signal was generated with the suspended PZT and collected with the epoxy-fastened PZT. No signal was recorded with the sound card, suggesting that the electromagnetic shielding was sufficient on the PZTs and that when the PZTs are fastened with epoxy to the quartz, they do not move unless driven by the excitation signal through mechanical contact. Second, where possible, support structures were made of wood to dampen sound. Wood is composed of a cellular network of pores that convert sound energy into heat by frictional and viscoelastic resistance.[40] Because of the high internal friction created by the cellular pore network, wood has more sound dampening capacity than most structural materials (eg, steel, aluminum, glass). Because the PZT and the sample support structures were made of wood, there was less sound traveling through the beams than if they had been made of metal. Additional sound dampening was accomplished by coupling the quartz rod to the support structure through rubber grommets. Finally, the support structure was

fixed in place and did not change during the experiment, so any sound traveling through it was the same for all sample and reference measurements. Third, spontaneous noise bursts (eg, lightning) from the receiver-generated noise might be a problem if they appeared sporadically in some tablet scans and not others. Such noises were eliminated by the use of FM and VHF frequencies. Fourth, 280 tablets were scanned without an anomalous spectrum because of manual tablet loading. A contoured sample holder helped to maintain reproducible sample positioning.[4]

Limits of Detection

The multidimensional population translation experiment[35] described in the Materials and Methods section was used to estimate the theoretical limits of detection. Using the populations with the smallest multidimensional separation (ibuprofen and aspirin), translation of one cluster toward the other indicated that tablets with a 0.08 mm difference in thickness, a 0.0046 g difference in mass, and a 0.01658 g/mL difference in density were no longer separable by ARS. This corresponds to a translation of one cluster 90% of the distance across hyperspace toward the other before the 2 begin to overlap (<3 SDs, ie, $P = .0013$). Using the populations with the largest multidimensional separation (acetaminophen and vitamin C), translation of one cluster toward the other indicated that tablets with a 0.27 mm difference in thickness, 0.0756 g difference in mass, and 0.01157 g/mL difference in density are inseparable. This corresponds to a translation of one cluster 93% of the distance across space toward the other before the 2 begin to overlap. From these experiments, the dynamic range for these properties appears to be about a factor of 10.

ARS may be useful within a PAT paradigm of networked sensors throughout a manufacturing process. The possibility of ISP[5,7] makes ARS a very attractive method for further investigation. An ISP-AR spectrometer now under construction employs a tailored excitation signal so the voltage at the detector becomes directly proportional to the desired analyte concentration or classification. When ARS becomes a standard sensor on a pharmaceutical manufacturing line, speed and accuracy of identification and quantification will be paramount. Collecting and processing full AR spectra for every sample can be too costly in terms of time, hardware, and computing power. ISP can preselect and weight excitation using only distinguishing frequencies, obviating the need for a full-spectrum approach. In this manner, the detector itself will provide the tablet identity signal without the need for postcollection chemometric interpretation. An ISP-AR spectrometer can be constructed from a CD or MP3 player, a simple, rugged device perfect for PAT. The sensor could be easily reprogrammed to analyze new

samples using CDs (or downloaded MP3s) with preprogrammed tracks consisting of calibration signals specifically written for different analytes and different properties.

Conclusion

This research suggests that ARS is a viable PAT for high-throughput tablet identification and characterization, because of its speed, performance, low cost, durability, versatility, and freedom from interferences. The FM receiver used as an excitation source in this research outperformed the FG, demonstrating that the most effective PAT sensor could be a very inexpensive instrument.

Acknowledgments

This research was supported in part by the US FDA through contract 200406251503, Science and Engineering Services Inc. and the National Institutes of Health through N01AA33003, and Kentucky Science and Engineering Foundation through 148-502-03-61.

References

1. US Food and Drug Administration. Magno-Humphries, Inc. voluntarily recalls one lot of Dixon's®, Acetaminophen 325 mg Analgesic, 100 Tablet bottles. Available at: http://www.fda.gov/oc/po/firmrecalls/magno12_03.html. Accessed April 1, 2005.

2. US Food and Drug Administration. Process Analytical Technology (PAT) Initiative. Available at: http://www.fda.gov/cder/OPS/PAT.htm. Accessed April 1, 2005.

3. Lu Z, Hickey C, Sabatier J. Effects of compaction on the acoustic velocity in soils. *Soil Sci Am J.* 2004;68:7-16.

4. Buice R, Pinkston P, Lodder R. Optimization of acoustic-resonance spectrometry for analysis of intact tablets and prediction of dissolution rate. *Appl Spectrosc*. 1994;48:517-524. DOI: 10.1366/000370294775268929

5. Medendorp J, Lodder RA. *Integrated Sensing and Processing and a Novel Acoustic-Resonance Spectrometer.* Baltimore, MD: American Association of Pharmaceutical Sciences; 2004.

6. Medendorp J, Lodder RA. Acoustic Resonance Spectrometry and Analysis of Powder Drying. Pittsburgh Conference on Analytical Chemistry and Applied Spectroscopy; March 7-12, 2004; Chicago, IL.

7. Medendorp J, Lodder RA. Applications of Integrated Sensing and Processing (ISP) in Acoustic and Optical Sceptroscopy. Pittsburgh Conference on Analytical Chemistry and Applied Spectroscopy; February 27-March 4, 2005; Orlando, FL.

8. Serris E, Camby-Perier L, Thomas G, Desfontaines M, Fantozzi G. Acoustic emission of pharmaceutical powders during compaction. *Powder Technol.* 2002;128:296-299.
DOI: 10.1016/S0032-5910(02)00174-2

9. Reynaud P, Dubois J, Rouby D, Fantozzi G. Acoustic emission monitoring of uniaxial pressing of ceramic powders. *Ceramics Int.* 1992;18:391-397.
DOI: 10.1016/0272-8842(92)90071-K

10. Martin L, Poret J, Danon A, Rosen M. Effect of adsorbed water on the ultrasonic velocity in alumina powder compacts. *Mater Sci Eng*. 1998;252:27-35.
DOI: 10.1016/S0921-5093(98)00669-8

11. Kaatze U, Wehrmann B, Pottel R. Acoustical absorption spectroscopy of liquids between 0.15 and 3000 MHz, I: high resolution ultrasonic resonator method. *J Phys E Sci Instrum*. 1987;20:1025-1030.
DOI: 10.1088/0022-3735/20/8/014

12. Bolotnikov M, Neruchev Y. Speed of sound of hexane + 1-chlorohexane, hexane + 1-iodohexane, and 1-chlorohexane + 1-iodohexane at saturation condition. *J Chem Eng Data*. 2003;48:411-415.
DOI: 10.1021/je0256129

13. Shah V, Tsong Y, Sathe P, Liu J. In vitro dissolution profile comparison-statistics and analysis of the similarity factor f2. *Pharm Res*. 1998;15:889-896.
PubMed DOI: 10.1023/A:1011976615750

14. Shah V, Williams R. Roles of dissolution testing: regulatory, industry, and academic perspectives. Available at: http://www.dissolutiontech.com/DTresour/899Art/Roles_Pt1.html/. Accessed March 15, 2005.

15. Drennen J, Lodder RA. Nondestructive near-infrared analysis of intact tablets for determination of degradation products. *J Pharm Sci*. 1990;79:622-627.
PubMed

16. Zannikos P, Li W, Drennen J, Lodder R. Spectrophotometric prediction of the dissolution rate of carbamazepine tablets. *Pharm Res*. 1991;8:974-978.
PubMed DOI: 10.1023/A:1015840604423

17. Dousseau F, Pezolet M. On the spectral subtraction of water from the FTIR spectra of aqueous solutions of proteins. *Appl Spectrosc*. 1989;43:538-543.
DOI: 10.1366/0003702894202814

18. Dousseau F, Pezolet M. Determination of the secondary structure content of proteins in aqueous solutions from their amide I and amide II infrared bands. *Biochemistry*. 1990;29:8771-8779.
PubMed DOI: 10.1021/bi00489a038

19. Maddams W, Southon M. The measurement of derivative IR spectra, III: the effect of band width and band shape on resolution enhancement by derivative spectroscopy. *Spectrochim Acta [A]*. 1982;38:459-466.
DOI: 10.1016/0584-8539(82)80022-6

20. Fleissner G, Hage W, Hallbrucker A, Mayer E. Improved curve resolution of highly overlapping bands by comparison of fourth-derivative curves. *Appl Spectrosc*. 1996;50:1235-1245.
DOI: 10.1366/0003702963904962

21. Cassis LA, Dai B, Urbas A, Lodder RA. In vivo applications of a molecular computing-based high-throughput NIR spectrometer. *Proc SPIE Int Soc Opt Eng.* 2004;239:5329-5344.

22. Kirmse D, Westerberg A. Resolution enhancement of chromatograph peaks. *Anal Chem*. 1971;43:1035-1039.
DOI: 10.1021/ac60303a002

23. Maldacker T, Davis J, Rogers L. Applications of Fourier transform techniques to steric-exclusion chromatography. *Anal Chem*. 1974;46:637-642.

DOI: 10.1021/ac60342a019

24. Buice RG, Jr, Lodder RA. Determination of cholesterol using a novel magnetohydrodynamic acoustic-resonance near-IR spectrometer. *Appl Spectrosc*. 1993;47:887-890.
DOI: 10.1366/0003702934415237

25. Ultrasonic Scientific. High Resolution Ultrasonic Spectroscopy for Material Characterization. Available at: http://www.ultrasonic-scientific.com. Accessed April 1, 2005.

26. Halliday D, Resnick R, Walker J. *Fundamentals of Physics.* New York, NY: Wiley; 2001.

27. Mills T, Jones A, Lodder R. Identification of wood species by acoustic-resonance spectrometry using multivariate subpopulation analysis. *Appl Spectrosc*. 1993;47:1880-1886.
DOI: 10.1366/0003702934065957

28. Ono Y, Jen CK, Cheng CC, Kobayashi M. Real time monitoring of injection molding for microfluidic devices using ultrasound. *Poly Eng Sci.* 2005;45:606-612.
DOI: 10.1002/pen.20310

29. Kowalska B. Ultrasonic measurements in polymeric processing. *Polimery.* 2005;50:646-650.

30. Moisan JF, Jen CK, Liaw JW, et al. Ultrasonic sensor and technique for in-line monitoring of die casting process. *Meas Sci Tech.* 2001;12:1956-1963.
DOI: 10.1088/0957-0233/12/11/327

31. Kilian & Co Inc. Product showcase for pharmaceutical manufacturing, pharmaceutical process technology engineering. Available at: http://www.pharmaceuticalonline.com/Content/ProductShowcase/product.asp?DocID={E21A91E3-9BB6-11D4-8C69-009027DE0829}&VNETCOOKIE=NO/. Accessed November 25, 2005.

32. Lodder R. CD/MP3 acoustic resonance spectrometer. Available at: http://www.pharm.uky.edu/. Accessed April 5, 2004.

33. Jolliffe IT. *Principal Component Analysis.* New York, NY: Springer; 2002.

34. Alves M, Oliveira M. Interpolative biplots applied to principal component analysis and canonical correlation analysis. *J Chemometr*. 2003;17:594-602.
DOI: 10.1002/cem.827

35. Hamilton S, Lodder R. Hyperspectral imaging technology for pharmaceutical analysis. *Proc Soc Photo-Optic Instrum Eng.* 2002;4626:136-147.

36. Lowell A, Ho K-S, Lodder RA. Remote hyperspectral imaging of endolithic biofilms using a robotic probe. *Contact Context.* 2002;1:1-10.

37. Buice R, Lodder RA. Determination of Cholesterol Using a Novel Magnetohydrodynamic Acostic-Resonance Near-IR (MARNIR) Spectrometer. *Appl Spectrosc*. 1993;47:887-890.
DOI: 10.1366/0003702934415237

38. Lai E, Chan B, Chen S. Ultrasonic resonance spectroscopic analysis of microliters of liquids. *Appl Spectrosc*. 1988;42:526-529.
DOI: 10.1366/0003702884427906

39. Ritter T. Random noise sources. Available at: http://www.ciphersbyritter.com/NOISE/NOISRC.HTM/. Accessed March 15, 2003.

40. Western Red Cedar Physical Properties. Available at: http://www.bearcreeklumber.com/generalinfo/onlineliterature/technicalinfohtml/wrcphysicalproperties.html/.

A publication of the American Association of Pharmaceutical Scientists

2107 Wilson Blvd., Suite 700, Arlington, Virginia, 22201, USA

703-243-2800, Fax: 703-243-9650, aaps@aaps.org